

Quarks and gluons in dense two-colour QCD

Jon-Ivar Skullerud

^a*Department of Mathematical Physics, NUI Maynooth, County Kildare, Ireland*

Abstract

We compute quark and gluon propagators in 2-colour QCD at large baryon chemical potential μ . The gluon propagator is found to be antiscreened at intermediate μ and screened at large μ . The quark propagator is drastically modified in the superfluid region as a result of the formation of a superfluid gap.

1. Introduction

Determining the phase diagram of QCD at large baryon density and small temperatures remains one of the outstanding problems of strong interaction physics. Direct lattice simulations of QCD at high density and low temperature are hindered by the sign problem, so alternative approaches are required. One such approach is to study QCD-like theories which may be simulated on the lattice, and apply the lessons learnt from these theories to the case of real QCD. Foremost among these theories is QCD with gauge group $SU(2)$ (QC_2D). Medium modifications of quark and gluon propagators is one topic where QC_2D may directly inform real QCD calculations. The gluon propagator is used as input into the gap equation for the superfluid gap at high density, and non-trivial medium modifications may significantly alter the results. First-principles results for gluon and quark propagators together can be used to check the assumptions going into dense QCD calculations in the Dyson–Schwinger equation framework [1,2].

We will be using $N_f = 2$ degenerate flavours of Wilson fermion, with a diquark source j included to lift low-lying eigenvalues and study diquark condensation without uncontrolled approximations. The fermion action can be written

$$S_F = \begin{pmatrix} \bar{\psi}_1 & \psi_2^T \end{pmatrix} \begin{pmatrix} M(\mu) & j\gamma_5 \\ -j\gamma_5 & M(-\mu) \end{pmatrix} \begin{pmatrix} \psi_1 \\ \bar{\psi}_2^T \end{pmatrix} \equiv \bar{\Psi} \mathcal{M}(\mu) \Psi, \quad (1)$$

where $M(\mu)$ is the usual Wilson fermion matrix with chemical potential μ . It satisfies the symmetries $KM(\mu)K^{-1} = M^*(\mu)$, $\gamma_5 M^\dagger(\mu) \gamma_5 = M(-\mu)$, with $K = C\gamma_5\tau_2$. The first of these is the Pauli–Gürsey symmetry. The inverse of \mathcal{M} is the Gor'kov propagator,

$$\mathcal{G}(x, y) = \mathcal{M}^{-1} = \begin{pmatrix} \langle \psi_1(x) \bar{\psi}_1(y) \rangle & \langle \psi_1(x) \psi_1^T(y) \rangle \\ \langle \bar{\psi}_2^T(x) \bar{\psi}_1(y) \rangle & \langle \bar{\psi}_2^T(x) \psi_1^T(y) \rangle \end{pmatrix} = \begin{pmatrix} S(x, y) & T(x, y) \\ \bar{T}(x, y) & \bar{S}(x, y) \end{pmatrix}. \quad (2)$$

The components S and T denote normal and anomalous propagation respectively. The normal (diagonal) part N of the inverse Gor'kov propagator can in general be written in terms of four momentum-space form factors,

$$N(p) = \not{p}A(\mathbf{p}^2, p_4) + B(\mathbf{p}^2, p_4) + \gamma_4(p_4 - i\mu)C(\mathbf{p}, p_4) + i\gamma_4 \not{p}D(\mathbf{p}^2, p_4). \quad (3)$$

Analogous form factors S_a, S_b, S_c, S_d can be written for the propagator S . In QC₂D the Pauli–Gürsey symmetry ensures that all form factors are purely real. Assuming that the condensation occurs in the colour singlet channel with quarks of unequal flavour, the anomalous propagator can be written as $T(p) = T'(p)C\Gamma\tau_2$ (and similarly for the anomalous part $A(p)$ of the inverse propagator), where $\Gamma = \gamma_5$ for condensation in the scalar (0^+) channel. The remaining spin structure can be written in terms of form factors T_a, T_b, T_c, T_d analogous to (3). The form factors $\phi_a, \phi_b, \phi_c, \phi_d$ for $A'(p)$ are the gap functions.

The gluon propagator in presence of a chemical potential in Landau gauge may be decomposed into an magnetic and electric form factor,

$$D_{\mu\nu}(\mathbf{q}, q_0) = P_{\mu\nu}^T D_M(\mathbf{q}^2, q_4^2) + P_{\mu\nu}^E D_E(\mathbf{q}^2, q_4^2). \quad (4)$$

The projectors $P_{\mu\nu}^T(q), P_{\mu\nu}^E(q)$ are both 4-dimensionally transverse, and are spatially transverse and longitudinal respectively.

2. Results

We have generated gauge configurations on two lattices: a “coarse” lattice with $\beta = 1.7, \kappa = 0.178, V = 8^3 \times 16$, and a “fine” lattice with $\beta = 1.9, \kappa = 0.168, V = 12^3 \times 24$. The lattice spacings are 0.23fm and 0.18fm respectively, while $m_\pi/m_\rho = 0.8$ in both cases. A range of chemical potentials μ were used with diquark source $aj = 0.04$, while additional configurations were generated with $aj = 0.02, 0.06$ for selected values of μ . Results for the gluon propagator on the coarse lattice have been presented in [3]; we will supplement these here with results from the fine lattice. On both lattices, an onset transition to a phase with nonzero baryon density and diquark condensate was found at $\mu_o \approx m_\pi/2$, while BCS-like scaling of energy density, baryon density and diquark condensate was found at higher μ . On the coarse lattice the crossover to BCS-like scaling was associated with a nonvanishing Polyakov loop L , indicating a coincident deconfinement transition [3]. On the fine lattice, this transition has been pushed to considerably larger μ [4].

Figure 1 shows the gluon propagator as a function of spatial momentum $|\mathbf{q}|$ for the two lowest Matsubara frequencies, on the fine lattice. In all cases, the propagator at the lowest chemical potential μ shown is consistent with the vacuum propagator. On the coarse lattice [3] both magnetic and electric propagator are strongly screened at large μ , while they are enhanced at low momentum in the intermediate-density region. On the fine lattice, the non-static modes of the magnetic propagator remain screened, while the static mode and the electric propagator experience much weaker modifications. The enhancement in the intermediate, superfluid region remains. The weaker screening may be linked to the deconfinement transition occurring at much higher μ , implying that the gluon is not screened by coloured quark degrees of freedom at these densities.

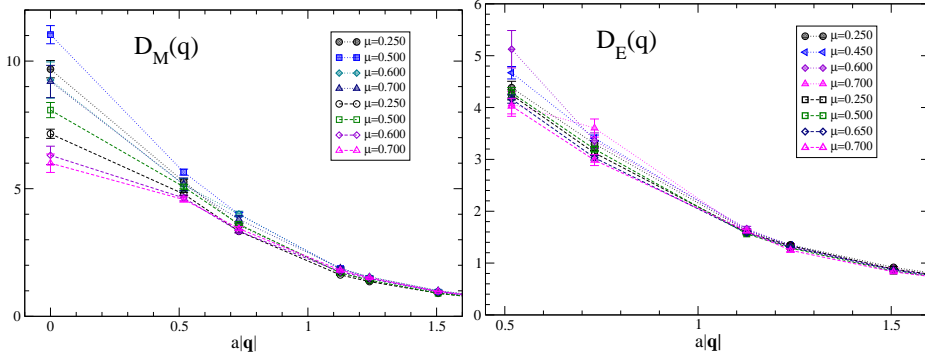


Fig. 1. Magnetic (left) and electric (right) gluon propagator on the fine lattice. The filled symbols represent the lowest Matsubara mode ($q_4 = 0$), while the open symbols represent the first nonzero Matsubara mode.

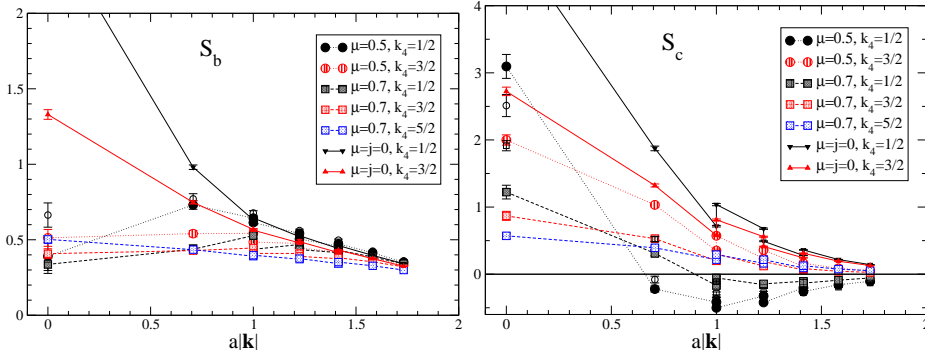


Fig. 2. The scalar (left) and temporal-vector (right) part of the normal quark propagator, on the coarse lattice. The filled symbols are for $a_j = 0.02$, while the open symbols are $a_j = 0.04$. The vacuum ($\mu = j = 0$) propagator is also shown for comparison.

Figure 2 shows the scalar part S_b and temporal-vector part S_c of the normal quark propagator for $a\mu = 0.5, 0.7$ on the coarse lattice. These both exhibit dramatic medium modifications. The scalar propagator S_b is strongly suppressed in the superfluid phase, suggesting a drastic reduction in the in-medium effective quark mass. This is linked to the appearance of the diquark condensate: the chiral condensate rotates into the diquark condensate in the superfluid phase [5]. We would therefore expect to find the missing strength in the anomalous propagator. The lowest Matsubara mode of S_c becomes negative at intermediate momenta, approaching zero from below at high momenta. This is a signal of a gap, and the location of the zero crossing in the $k_0 \rightarrow 0$ limit can be used to determine the Fermi momentum. In accordance with this, the zero crossing moves to larger $|\mathbf{k}|$ as μ increases. The spatial-vector propagator S_a experiences smaller modifications, while the tensor part S_d is found to be consistent with zero. Preliminary results from the fine lattice confirm this picture.

Figure 3 shows the nonzero components of the anomalous Gor'kov propagator. The dominant part is, as expected, the scalar part T_b , but a clear signal is also found for the tensor part T_d . There is also a non-zero signal for the lowest Matsubara frequency of the temporal-vector propagator T_c . Neither the normal nor the anomalous propagator

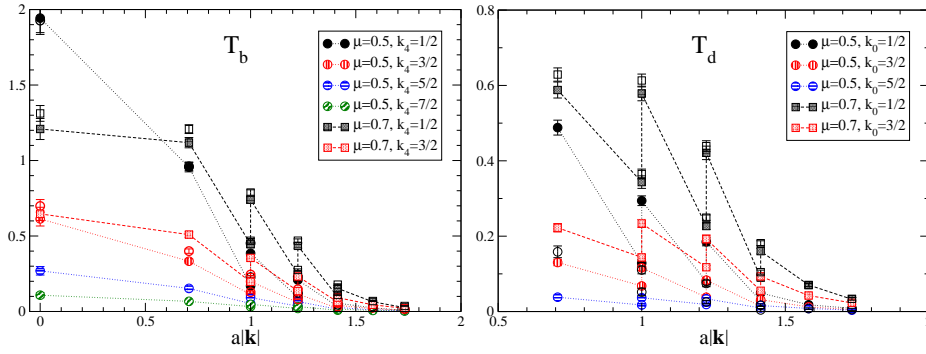


Fig. 3. The scalar (left) and tensor (right) part of the anomalous quark propagator, on the coarse lattice. The filled symbols are for $aj = 0.02$, while the open symbols are $aj = 0.04$.

depend strongly on the diquark source term j . Lattice artefacts are however quite large, as indicated by the discrepancy between the two points at $a|\mathbf{k}| = 1$. Quantitative results will require analysis of the quark propagator on the fine lattice.

3. Discussion and outlook

We have found substantial modifications of both gluon and quark propagators in the dense medium. Both electric and magnetic gluon propagator are screened at large μ , but a more quantitative analysis, including extrapolation to $j = 0$ and fits to determine screening masses, will be necessary to draw firm conclusions. Note that the gluon propagator is known to be infrared suppressed in the vacuum [6–8], so even without further medium modifications the static magnetic gluon propagator will be screened, in contradiction to any perturbative approximation.

The dramatic modifications seen in the quark propagator are directly related to the appearance of a diquark gap. Further quantitative studies of this will include determining the Fermi momentum p_F from $S_c(p_F, k_A = 0) = 0$ and determining the size of Cooper pairs from the anomalous propagator, to study the BEC–BCS crossover in more detail.

Acknowledgments

I wish to thank Simon Hands for his collaboration in this research, and Dominik Nickel for very fruitful discussions.

References

- [1] C.D. Roberts and S.M. Schmidt, Prog. Part. Nucl. Phys. 45S1 (2000) 1 [nucl-th/0005064].
- [2] D. Nickel, J. Wambach and R. Alkofer, Phys. Rev. D73 (2006) 114028 [hep-ph/0603163].
- [3] S. Hands, S. Kim and J.I. Skullerud, Eur. Phys. J. C48 (2006) 193 [hep-lat/0604004].
- [4] S. Hands, private communication.
- [5] J. Kogut et al., Nucl. Phys. B582 (2000) 477 [hep-ph/0001171].
- [6] D.B. Leinweber et al., Phys. Rev. D58 (1998) 031501 [hep-lat/9803015].
- [7] A. Cucchieri and T. Mendes, PoS LAT2007 (2007) 297 [0710.0412].
- [8] I.L. Bogolubsky et al., PoS LAT2007 (2007) 290 [0710.1968].